

One-Dimensional Numerical Model for Nonuniform Sediment Transport under Unsteady Flows in Channel Networks

Weiming Wu, M.ASCE¹; Dalmo A. Vieira²; and Sam S. Y. Wang, F.ASCE³

Abstract: In this study, the proposed one-dimensional model simulates the nonequilibrium transport of nonuniform total load under unsteady flow conditions in dendritic channel networks with hydraulic structures. The equations of sediment transport, bed changes, and bed-material sorting are solved in a coupling procedure with a direct solution technique, while still decoupled from the flow model. This coupled model for sediment calculation is more stable and less likely to produce negative values for bed-material gradation than the traditional fully decoupled model. The sediment transport capacity is calculated by one of four formulas, which have taken into consideration the hiding and exposure mechanism of nonuniform sediment transport. The fluvial erosion at bank toes and the mass failure of banks are simulated to complement the modeling of bed morphological changes in channels. The tests in several cases show that the present model is capable of predicting sediment transport, bed changes, and bed-material sorting in various situations, with reasonable accuracy and reliability.

DOI: 10.1061/(ASCE)0733-9429(2004)130:9(914)

CE Database subject headings: Numerical models; Unsteady flow; Sediment transport; Open channels; Hydraulic structures.

Introduction

One-dimensional (1-D) modeling of sediment transport in streams has seen extensive development over the past decades. Steady and stepwise quasisteady 1-D models, such as HEC-6 (Thomas 1982), Han's (1980) model, Chang's (1982) model, van Niekerk et al.'s (1992) model and others, have been widely tested and applied to sedimentation studies in reservoirs and rivers in which the long wave assumption is valid and the long-term results are mainly considered. Many unsteady flow models (e.g., Cunge et al. 1980; Tsai and Yen 1982; Rahuel et al. 1989) have been developed and applied to river estuaries and other situations where the unsteadiness of flow prevails. With a lot of enhancement and refinement, 1-D models continue to have their place in engineering applications.

The majority of the early 1-D sediment transport models decoupled the flow and sediment calculations, which resulted in simpler computer codes. This strategy was justified because of the different time scales of flow and sediment transport and the inherent inaccuracies introduced by the use of empirical formulas for bed roughness and sediment transport capacity. Recently, much effort has been made toward relaxing the limit in time and

space steps and extending the applicability of the fully decoupled model. One effective approach is to couple the equations of flow and sediment movement, which was done by Lyn and Goodwin (1987), Holly and Rahuel (1990), Lai (1991), Correia et al. (1992), Cui et al. (1996), Kassem and Chaudhry (1998), and others. Saiedi (1997) and Cao et al. (2002) compared the numerical stability of coupled and decoupled models and found out that the coupled model is more stable. However, the implementation of a coupled model for nonuniform sediment transport is rather complicated, which is one of the reasons the decoupled models are still used by many scientists.

Another approach, which has substantially improved sediment transport modeling, is the nonequilibrium (also referred as non-saturated) sediment transport model (Han 1980; Bell and Sutherland 1983; Armanini and di Silvio 1988; Phillips and Sutherland 1989; Rahuel et al. 1989; Wu, Rodi, and Wenka 2000). In the traditional equilibrium (or saturated) transport model, the actual sediment transport rate is assumed equal to the sediment transport capacity at every cross section (i.e., locally at equilibrium state), and the bed change is calculated by the sediment continuity equation. However, in many cases, such as sediment strongly overloading or underloading, the inflow sediment discharge imposed at the inlet is significantly different from the transport capacity, which might lead to difficulties in the calculation of bed changes near the inlet, thus requiring a small time step. The nonequilibrium transport model adopts the mass transport equation to determine the actual sediment transport rate, which should be more suitable for the simulation of sediment transport in natural rivers that are mostly in nonequilibrium state.

In the present study, a 1-D model is established for the long-term simulation of the unsteady flow and the nonequilibrium, nonuniform sediment transport in channel networks. A semi-coupled model is proposed in which the sediment computations are decoupled from the flow calculations, but the equations of sediment transport, bed changes, and bed-material sorting in the sediment module are solved using a coupling scheme that does not require iterations. Introduced here are the physical principles,

¹Research Assistant Professor, National Center for Computational Hydroscience and Engineering (NCCHE), The Univ. of Mississippi, University, MS 38677. E-mail: wuwm@ncche.olemiss.edu

²Research Associate, NCCHE, The Univ. of Mississippi, University, MS 38677. E-mail: dalmo@ncche.olemiss.edu

³F.A.P. Barnard Distinguished Professor and Director, NCCHE, The Univ. of Mississippi, University, MS 38677. E-mail: wang@ncche.olemiss.edu

Note. Discussion open until February 1, 2005. Separate discussions must be submitted for individual papers. To extend the closing date by one month, a written request must be filed with the ASCE Managing Editor. The manuscript for this paper was submitted for review and possible publication on December 17, 2002; approved on March 26, 2004. This paper is part of the *Journal of Hydraulic Engineering*, Vol. 130, No. 9, September 1, 2004. ©ASCE, ISSN 0733-9429/2004/9-914-923/\$18.00.

numerical methods, parameter sensitivity analyses, and several selected test cases of the proposed model.

One-Dimensional Hydrodynamic Model

Governing Equations for Open-Channel Flows

The governing equations of the 1-D dynamic wave model for open-channel flows with low-concentration sediment are the St. Venant equations

$$\frac{\partial A}{\partial t} + \frac{\partial Q}{\partial x} = q \quad (1)$$

$$\frac{\partial}{\partial t} \left(\frac{Q}{A} \right) + \frac{\partial}{\partial x} \left(\frac{\beta Q^2}{2A^2} \right) + g \frac{\partial y}{\partial x} + g S_f = 0 \quad (2)$$

where x and t =spatial and temporal axes; A =flow area; Q =flow discharge; y =water surface elevation; β =correction factor due to the nonuniformity of velocity distribution in the cross section; g =gravitational acceleration; q =side discharge per unit channel length; and S_f =friction slope, defined as $S_f = Q|Q|/K^2$, with K being the conveyance.

When the hydraulic properties in main channel and flood plains are noticeably different, the cross section is divided into three subsections: a main channel, and optional right and left flood plains. The conveyance K for the entire cross section is determined as $K = \sum_{l=1}^3 A_l R_l^{2/3} / n_l$, in which A_l , R_l , and n_l are, respectively, the flow area, hydraulic radius, and Manning's roughness coefficient of subsection l . However, the Manning's n is stored at each node in the cross section, so that the model is also able to calculate K for the channels with more complex geometry, such as braided channels.

Discretization of Governing Equations by Preissmann's Scheme

The implicit four-point finite difference scheme proposed by Preissmann (1961) is used to discretize the governing Eqs. (1) and (2) as

$$\begin{aligned} & \frac{\psi}{\Delta t} (A_{j+1}^{n+1} - A_{j+1}^n) + \frac{1-\psi}{\Delta t} (A_j^{n+1} - A_j^n) + \frac{\theta}{\Delta x} (Q_{j+1}^{n+1} - Q_j^{n+1}) \\ & + \frac{1-\theta}{\Delta x} (Q_{j+1}^n - Q_j^n) - \theta [\psi q_{j+1}^{n+1} + (1-\psi) q_j^{n+1}] \\ & - (1-\theta) [\psi q_{j+1}^n + (1-\psi) q_j^n] = 0 \end{aligned} \quad (3)$$

$$\begin{aligned} & \frac{\psi}{\Delta t} \left(\frac{Q_{j+1}^{n+1}}{A_{j+1}^{n+1}} - \frac{Q_{j+1}^n}{A_{j+1}^n} \right) + \frac{1-\psi}{\Delta t} \left(\frac{Q_j^{n+1}}{A_j^{n+1}} - \frac{Q_j^n}{A_j^n} \right) \\ & + \frac{\theta}{\Delta x} \left[\frac{\beta_{j+1}^{n+1}}{2} \left(\frac{Q_{j+1}^{n+1}}{A_{j+1}^{n+1}} \right)^2 - \frac{\beta_j^{n+1}}{2} \left(\frac{Q_j^{n+1}}{A_j^{n+1}} \right)^2 \right] \\ & + \frac{1-\theta}{\Delta x} \left[\frac{\beta_{j+1}^n}{2} \left(\frac{Q_{j+1}^n}{A_{j+1}^n} \right)^2 - \frac{\beta_j^n}{2} \left(\frac{Q_j^n}{A_j^n} \right)^2 \right] + \frac{\theta g}{\Delta x} (y_{j+1}^{n+1} - y_j^{n+1}) \\ & + \frac{(1-\theta)g}{\Delta x} (y_{j+1}^n - y_j^n) + \theta g [\psi S_{f,j+1}^{n+1} + (1-\psi) S_{f,j}^{n+1}] \\ & + (1-\theta) g [\psi S_{f,j+1}^n + (1-\psi) S_{f,j}^n] = 0 \end{aligned} \quad (4)$$

where superscript n and subscript j denote the numbers of time and space steps, respectively; Δt and Δx =step lengths in time and space, respectively; θ and ψ =temporal and spatial factors in Preissmann's scheme, respectively, with ψ usually being given as 0.5 and θ being in the range of 0.5 and 1 (Lyn and Goodwin 1987); ψ_R =spatial factor for friction slope in the case of small flow depth. The weighting of the friction slope in the case of small depth in natural streams is switched from central ($\psi_R = 0.5$) to upstream ($0 \leq \psi_R \leq 0.5$) in order to overcome the dry-bed problem, in which, as the flow depth approaches zero, the conveyance and flow discharge also go to zero, and the friction slope becomes indeterminate (Cunge et al. 1980; Meselhe and Holly 1993; Langendoen 1996).

Linearization and Iteration Scheme

Because Eq. (4) is nonlinear, an iteration method is needed to solve Eqs. (3) and (4). During the iteration process, one may assume $A_j^{n+1} = A_j^* + \Delta A_j = A_j^* + B_j^* \Delta h_j$, and $Q_j^{n+1} = Q_j^* + \Delta Q_j$, in which $*$ denotes variable values at the last iteration step, ΔA , Δh , and ΔQ are the increments of flow area, depth, and discharge, respectively, to be determined, and B is the channel width at water surface. Substituting these two relations into Eqs. (3) and (4) and linearizing the nonlinear terms, one can obtain the following iteration relations:

$$a_j \Delta h_j + b_j \Delta Q_j + c_j \Delta h_{j+1} + d_j \Delta Q_{j+1} + p_j = 0 \quad (5)$$

$$e_j \Delta h_j + f_j \Delta Q_j + g_j \Delta h_{j+1} + w_j \Delta Q_{j+1} + r_j = 0 \quad (6)$$

where a_j , b_j , c_j , d_j , e_j , f_j , g_j , and w_j =coefficients; and p_j and r_j =residues of Eqs. (3) and (4) at each iteration step.

The pentadiagonal matrix described by Eqs. (5) and (6) is solved by successively applying a double sweep algorithm, the Thomas algorithm, to obtain Δh and ΔQ at each iteration step. The flow depth h^* and discharge Q^* are then updated by $h^* + \Delta h$ and $Q^* + \Delta Q$. The iteration performed at each time step is stopped when $\Delta h \rightarrow 0$ and $\Delta Q \rightarrow 0$. Usually, this solution method is convergent within a few iteration steps.

The present model considers the effect of hydraulic structures, such as culverts, bridge crossings, drop structures, and measuring flumes. The flow-discharge balance equation and the stage-discharge relation for each structure are expanded as first-order Taylor's series, which are rewritten in forms of Eqs. (5) and (6), and then included into the above solution algorithm as an intrinsic part. Details refer to Wu and Vieira (2002).

One-Dimensional Sediment Transport Model

Governing Equations for Sediment Transport

Unifying the nonequilibrium bed-load transport model of Phillips and Sutherland (1989), the suspended-load transport model of Han (1980), and the total-load model of Armanini and di Silvio (1988) leads to the governing equation for the nonequilibrium transport of nonuniform sediment

$$\frac{\partial (AC_{tk})}{\partial t} + \frac{\partial Q_{tk}}{\partial x} + \frac{1}{L_s} (Q_{tk} - Q_{t^*k}) = q_{tk} \quad (7)$$

where C_{tk} =section-averaged sediment concentration of size class k ; Q_{tk} =actual sediment transport rate; Q_{t^*k} =sediment transport capacity or the so-called equilibrium transport rate; L_s =nonequilibrium adaptation length of sediment transport; and

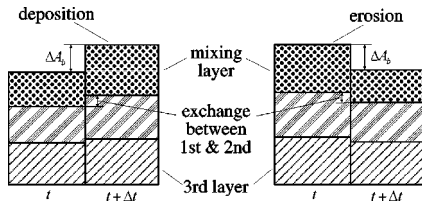


Fig. 1. Multiple-layer model for bed-material sorting

q_{lk} = side inflow or outflow sediment discharge from bank boundaries or tributary streams per unit channel length.

The first term on the left-hand side of Eq. (7) accounts for the storage effect, while the last term on the left-hand side represents the exchanges between the moving sediment and the bed material, with Q_{tk}/L_s and $Q_{t* k}/L_s$ representing deposition and erosion, respectively. Eq. (7) can be applied to bed load and suspended load separately, or to bed-material load and wash load, depending on how the sediment transport rate and the adaptation length are defined. For example, defining $L_s = Uh/(\alpha \omega_{sk})$, $Q_{tk} = QC_{tk}$, and $Q_{t* k} = QC_{t* k}$, one can rewrite Eq. (7) as the commonly used suspended-load transport equation with the exchange term $\alpha \omega_{sk} B(C_{tk} - C_{t* k})$. Here, U is the section-averaged velocity, h is the flow depth, ω_{sk} is the settling velocity of sediment particles, α is the nonequilibrium adaptation coefficient or the recovery coefficient, and $C_{t* k}$ is the suspended-load transport capacity. In this paper, the proposed model does not distinguish bed load and suspended load, but treats them together as bed-material load. Therefore, Eq. (7) is applied to the bed-material load, where the transport rate Q_{tk} is the sum of bed-load and suspended-load transport rates. Eq. (7) is also applied to wash load, where the adaptation length L_s is assumed to be infinitely large and then the exchange term on the left-hand side is zero. The wash-load size range is determined with the Rouse number $\omega_{sk}/\kappa u_* < 0.06$. Here, κ is the von Karman constant and u_* is the shear velocity.

The sediment transport capacity can be written as a general form

$$Q_{t* k} = p_{bk} Q_{tk}^* \quad (8)$$

where p_{bk} = availability factor of sediment, which is defined as the bed-material gradation in the mixing layer here; and Q_{tk}^* = potential sediment transport capacity for size class k , which can be determined with the help of empirical relations that are given later.

The bed deformation due to size class k is determined with

$$(1 - p') \left(\frac{\partial A_b}{\partial t} \right)_k = \frac{1}{L_s} (Q_{tk} - Q_{t* k}) \quad (9)$$

where p' = bed-material porosity; and $(\partial A_b / \partial t)_k$ = bed deformation rate of size class k . In fact, combining Eqs. (7) and (9) leads to the sediment continuity equation, which could also be used to calculate the bed deformation. However, it has more spatial-derivative terms than Eq. (9) and thus needs more computational nodes in the numerical discretization.

The bed material is divided into several layers to allow the computation of changes in bed-material gradation due to erosion or deposition, as shown in Fig. 1. According to mass balance, Wu (1991) derived the following equation for the variation of bed-material gradation at the mixing layer (surface layer):

$$\frac{\partial (A_m p_{bk})}{\partial t} = \left(\frac{\partial A_b}{\partial t} \right)_k + p_{bk}^* \left(\frac{\partial A_m}{\partial t} - \frac{\partial A_b}{\partial t} \right) \quad (10)$$

where p_{bk} = bed-material gradation at the mixing layer; A_m = cross-sectional area of mixing layer, whose thickness is set as half the sand dune height calculated with van Rijn's (1984) formula in general, but given as the median size of bed material for channel armoring; $\partial A_b / \partial t$ = total bed deformation rate, $\partial A_b / \partial t = \sum_{k=1}^N (\partial A_b / \partial t)_k$; N = total number of size classes; p_{bk}^* is p_{bk} when $\partial A_m / \partial t - \partial A_b / \partial t \leq 0$; and p_{bk}^* = bed-material gradation at the subsurface layer (below the mixing layer) when $\partial A_m / \partial t - \partial A_b / \partial t > 0$. The last term on the right-hand side represents the exchange between the mixing layer and subsurface layer.

Discretization of Governing Equations

The depth-averaged sediment concentration and the sediment transport rate can be expressed as $C_{tk} = Q_{tk} / (\beta_s A U)$, in which β_s is a coefficient accounting for the difference between flow and sediment velocities that may produce time lags, and is assumed to be 1 here. Substituting this relation into Eq. (7) and discretizing it using Preissmann's implicit scheme leads to

$$c_1 Q_{tk,j+1}^{n+1} = c_2 Q_{tk,j}^{n+1} + c_3 Q_{tk,j+1}^n + c_4 Q_{tk,j}^n + c_{0k} \quad (11)$$

where

$$\begin{aligned} c_1 &= \frac{\psi}{U_{j+1}^{n+1} \Delta t} + \frac{\theta}{\Delta x} + \frac{\theta \psi}{L_{s,j+1}^{n+1}} \\ c_2 &= -\frac{1-\psi}{U_j^{n+1} \Delta t} + \frac{\theta}{\Delta x} - \frac{\theta(1-\psi)}{L_{s,j}^{n+1}} \\ c_3 &= \frac{\psi}{U_{j+1}^n \Delta t} - \frac{1-\theta}{\Delta x} - \frac{(1-\theta)\psi}{L_{s,j+1}^n} \\ c_4 &= \frac{1-\psi}{U_j^n \Delta t} + \frac{1-\theta}{\Delta x} - \frac{(1-\theta)(1-\psi)}{L_{s,j}^n} \\ c_{0k} &= \theta \psi \frac{Q_{t* k,j+1}^{n+1}}{L_{s,j+1}^{n+1}} + \theta(1-\psi) \frac{Q_{t* k,j}^{n+1}}{L_{s,j}^{n+1}} + (1-\theta) \psi \frac{Q_{t* k,j+1}^n}{L_{s,j+1}^n} \\ &\quad + (1-\theta)(1-\psi) \frac{Q_{t* k,j}^n}{L_{s,j}^n} + \theta \psi q_{lk,j+1}^{n+1} + \theta(1-\psi) q_{lk,j}^{n+1} \\ &\quad + (1-\theta) \psi q_{lk,j+1}^n + (1-\theta)(1-\psi) q_{lk,j}^n \end{aligned}$$

In fact, many higher-order numerical schemes in the literature can be used to solve Eq. (7). However, more computational nodes in space or in time will be involved and more computation time will be needed. Preissmann's implicit scheme is simple and efficient. The use of this scheme can also be justified by the accuracy of the empirical formulas for sediment transport capacity, which may have errors of $\pm 100\%$ or larger.

Since the calculation of sediment transport is carried out from upstream node j to downstream node $j+1$, only $Q_{tk,j+1}^{n+1}$ and $Q_{t* k,j+1}^{n+1}$ are unknowns in Eq. (11). For the convenience of analysis in the next section, Eq. (11) is also written as

$$Q_{tk,j+1}^{n+1} = e_k Q_{t* k,j+1}^{n+1} + e_{0k} \quad (12)$$

where $e_k = \theta \psi / (c_1 L_{s,j+1}^{n+1})$; $e_{0k} = (c_2 Q_{tk,j}^{n+1} + c_3 Q_{tk,j+1}^n + c_4 Q_{tk,j}^n + c_{0k} - \theta \psi Q_{t* k,j+1}^{n+1} / L_{s,j+1}^{n+1}) / c_1$. e_k and e_{0k} include all the known parameters.

In order to satisfy the sediment continuity, the right-hand side

of Eq. (9) is discretized with the same scheme as the exchange term in Eq. (7), expressed as

$$(1-p') \frac{\Delta A_{bk,j+1}}{\Delta t} = \theta \frac{Q_{tk,j+1}^{n+1} - Q_{tk,j+1}^{n+1}}{L_{s,j+1}^{n+1}} + (1-\theta) \frac{Q_{tk,j+1}^n - Q_{tk,j+1}^n}{L_{s,j+1}^n} \quad (13)$$

where $\Delta A_{bk,j+1}$ = bed deformation corresponding to size class k at the time step Δt .

Eq. (13) can be rewritten as

$$\Delta A_{bk,j+1} = f_1 Q_{tk,j+1}^{n+1} - f_2 Q_{tk,j+1}^{n+1} + f_{0k} \quad (14)$$

where $f_1 = f_2 = \theta \Delta t / [(1-p') L_{s,j+1}^{n+1}]$; $f_{0k} = (1-\theta) \Delta t (Q_{tk,j+1}^n - Q_{tk,j+1}^{n+1}) / [(1-p') L_{s,j+1}^n]$.

Eq. (8) is expressed with an implicit scheme

$$Q_{tk,j+1}^{n+1} = p_{bk,j+1}^{n+1} Q_{tk,j+1}^{*n+1} \quad (15)$$

Eq. (10) of bed-material sorting in the mixing layer is discretized as

$$p_{bk,j+1}^{n+1} = \frac{\Delta A_{bk,j+1} + A_{m,j+1}^n p_{bk,j+1}^n + p_{bk,j+1}^{*n} (A_{m,j+1}^{n+1} - A_{m,j+1}^n - \Delta A_{b,j+1})}{A_{m,j+1}^{n+1}} \quad (16)$$

where $p_{bk,j+1}^{*n}$ is defined as $p_{bk,j+1}^n$, if $\Delta A_{b,j+1} + A_{m,j+1}^n \geq A_{m,j+1}^{n+1}$, and $p_{bk,j+1}^{*n}$ is the bed-material gradation in the subsurface layer, if $\Delta A_{b,j+1} + A_{m,j+1}^n < A_{m,j+1}^{n+1}$; and $\Delta A_{b,j+1}$ is the total bed deformation, expressed as

$$\Delta A_{b,j+1} = \sum_{k=1}^N \Delta A_{bk,j+1} \quad (17)$$

The bed-material gradation for the layers below the mixing layer is calculated according to mass conservation.

Solution of Algebraic Equations

If $p_{bk,j+1}^{*n+1}$ in Eq. (15) is replaced by $p_{bk,j+1}^n$, an assumption adopted by most of the sediment transport models, the calculation can proceed successively through Eqs. (12) and (14)–(17), thus forming a fully decoupling method for the solution of the algebraic equations. This method is very simple, but it is susceptible to the development of nonphysical phenomena, such as numerical oscillations and negative bed-material gradation. Instead, the term $p_{bk,j+1}^{*n+1}$ in Eq. (15) is treated implicitly, which establishes a coupling method for the solution of nonuniform sediment transport, bed deformation, and bed-material sorting. This method is more likely to eliminate the aforementioned problems, as it will be demonstrated later.

However, the set of algebraic Eqs. (12) and (14)–(17) must be solved simultaneously. Normally, an iteration method would be needed and the computation time would increase considerably. In order to avoid increasing the computation effort, a direct solution method is adopted. By inserting Eqs. (12) and (15) into Eq. (14), one can obtain

$$\Delta A_{bk,j+1} = (f_1 e_k - f_2) p_{bk,j+1}^{n+1} Q_{tk,j+1}^{*n+1} + (f_1 e_{0k} + f_{0k}) \quad (18)$$

then inserting Eq. (16) into Eq. (18) yields

$$\Delta A_{bk,j+1} = \Delta A_{b,j+1} \frac{(f_2 - f_1 e_k) Q_{tk,j+1}^{*n+1} p_{bk,j+1}^{*n}}{A_{m,j+1}^{n+1} + (f_2 - f_1 e_k) Q_{tk,j+1}^{*n+1}} + \frac{(f_1 e_{0k} + f_{0k}) A_{m,j+1}^{n+1}}{A_{m,j+1}^{n+1} + (f_2 - f_1 e_k) Q_{tk,j+1}^{*n+1}} - \frac{(f_2 - f_1 e_k) Q_{tk,j+1}^{*n+1} [p_{bk,j+1}^n A_{m,j+1}^n + p_{bk,j+1}^{*n} (A_{m,j+1}^{n+1} - A_{m,j+1}^n)]}{A_{m,j+1}^{n+1} + (f_2 - f_1 e_k) Q_{tk,j+1}^{*n+1}} \quad (19)$$

Summing Eq. (19) over all size classes and using Eq. (17), one can obtain the following equation to directly calculate the total bed deformation:

$$\Delta A_{b,j+1} = \left\{ - \sum_{k=1}^N \frac{(f_2 - f_1 e_k) Q_{tk,j+1}^{*n+1} [p_{bk,j+1}^n A_{m,j+1}^n + p_{bk,j+1}^{*n} (A_{m,j+1}^{n+1} - A_{m,j+1}^n)]}{A_{m,j+1}^{n+1} + (f_2 - f_1 e_k) Q_{tk,j+1}^{*n+1}} + \sum_{k=1}^N \frac{(f_1 e_{0k} + f_{0k}) A_{m,j+1}^{n+1}}{A_{m,j+1}^{n+1} + (f_2 - f_1 e_k) Q_{tk,j+1}^{*n+1}} \right\} \left/ \left[1 - \sum_{k=1}^N \frac{(f_2 - f_1 e_k) Q_{tk,j+1}^{*n+1} p_{bk,j+1}^{*n}}{A_{m,j+1}^{n+1} + (f_2 - f_1 e_k) Q_{tk,j+1}^{*n+1}} \right] \right. \quad (20)$$

After $\Delta A_{b,j+1}$ is calculated by Eq. (20), the fractional bed deformation $\Delta A_{bk,j+1}$ can be calculated by Eq. (19), $p_{bk,j+1}^{n+1}$ by Eq. (16), $Q_{tk,j+1}^{n+1}$ by Eq. (15), and $Q_{tk,j+1}^{*n+1}$ by Eq. (12), in a sequence. When compared to the fully decoupled model, the computation effort required by the proposed coupled model is increased only by the computation of Eq. (20). Because the coupled approach is much more stable, a larger time step Δt can be used for the sediment calculation, which by far offsets the computation time spent for Eq. (20) and significantly increases the overall computation efficiency.

Boundary Conditions of Sediment Transport

For the sediment transport calculation, the inflow sediment discharges for all size fractions must be given at upstream inlet nodes and at those nodes having lateral inflow. At any channel confluence, the sediment discharge in the downstream branch is the sum of the sediment discharges in the two upstream branches.

For hydraulic structures with nonerodible beds, such as culverts, drop structures, and measuring flumes, erosion and deposition are not allowed. Hence, the bed is fixed and the sediment discharges at the upstream and downstream ends of the structure are equal.

Properties of the Numerical Methods

The numerical stability of Preissmann's implicit scheme for the St. Venant equations has been studied by Lyn and Goodwin (1987) and Venutelli (2002). Here, a detailed analysis is done for the sediment model equations.

Stability of Preissmann's Scheme for Sediment Transport Equation

Neglecting the influence of the source term in Eq. (11), the error equation of the actual sediment transport rate corresponding to Eq. (11) is

$$c_1 \delta_{j+1}^{n+1} = c_2 \delta_j^{n+1} + c_3 \delta_{j+1}^n + c_4 \delta_j^n \quad (21)$$

where δ_j^n = Fourier component defined as $\delta_j^n = V^n e^{i\sigma x_j}$, with V^n and σ being the amplitude and wave number, respectively, of the Fourier component. Inserting the definition expression of δ_j^n into Eq. (21), one can obtain the growth factor

$$G = \frac{V^{n+1}}{V^n} = \frac{c_3 e^{i\sigma \Delta x} + c_4}{c_1 e^{i\sigma \Delta x} - c_2} \quad (22)$$

The coefficients of Eq. (11) satisfy that $c_1 \geq 0$ and $c_2 + c_3 + c_4 \leq c_1$ if the velocity does not change sharply. Supposing c_2 , c_3 , and $c_4 \geq 0$, we have

$$|G| = \left| \frac{c_3 e^{i\sigma \Delta x} + c_4}{c_1 e^{i\sigma \Delta x} - c_2} \right| = \left| \frac{c_3 + c_4 e^{-i\sigma \Delta x}}{c_1 - c_2 e^{-i\sigma \Delta x}} \right| \leq \frac{c_3 + c_4}{c_1 - c_2} \leq 1 \quad (23)$$

which means that the von Neumann condition is satisfied and the numerical scheme is stable. For a homogeneous case, in which U and L_s are constant in the element ($j \rightarrow j+1, n \rightarrow n+1$), the constraints c_2 , c_3 , and $c_4 \geq 0$ imply

$$\max \left\{ 1 - \frac{\psi}{C + \psi D_r}, \frac{1 - \psi}{C - (1 - \psi) D_r} \right\} \leq \theta \leq 1, \quad \text{with } \max \left\{ 0, 1 - \frac{C}{D_r} \right\} \leq \psi \leq 1 \quad (24)$$

where C = Courant number, $C = U \Delta t / \Delta x$; and D_r = scale factor to account for the nonequilibrium transport of sediment, $D_r = U \Delta t / L_s$.

Condition (24) is sufficient but not necessary for the numerical stability of scheme (11). Because $C/D_r = L_s / \Delta x$, if $L_s \ll \Delta x$, then ψ and θ should be given values close to 1.

Stability of Implicit and Explicit Schemes for Bed-Material Gradation

The numerical stability of the implicit scheme for bed-material gradation $p_{bk,j+1}^{n+1}$ in Eq. (15) is analyzed by comparing it with

that for the explicit scheme. For the convenience of this comparative analysis, Eq. (15) is replaced by

$$Q_{tk,j+1}^{n+1} = [\theta_p p_{bk,j+1}^{n+1} + (1 - \theta_p) p_{bk,j+1}^n] Q_{tk,j+1}^{*n+1} \quad (25)$$

where θ_p is the temporal factor for bed-material gradation. $\theta_p = 1$ for the implicit scheme, and $\theta_p = 0$ for the explicit scheme.

From Eqs. (12), (14), (16), and (25), one can obtain the equation for bed-material gradation as follows:

$$p_{bk,j+1}^{n+1} = \frac{(A_{m,j+1}^{n+1} - A_{m,j+1}^n - \Delta A_{b,j+1}) p_{bk,j+1}^{*n+1}}{A_{m,j+1}^{n+1} + (f_2 - f_1 e_k) \theta_p Q_{tk,j+1}^{*n+1}} + \frac{[A_{m,j+1}^n - (f_2 - f_1 e_k)(1 - \theta_p) Q_{tk,j+1}^{*n+1}] p_{bk,j+1}^n}{A_{m,j+1}^{n+1} + (f_2 - f_1 e_k) \theta_p Q_{tk,j+1}^{*n+1}} + \frac{f_1 e_{0k} + f_{0k}}{A_{m,j+1}^{n+1} + (f_2 - f_1 e_k) \theta_p Q_{tk,j+1}^{*n+1}} \quad (26)$$

To simplify the analysis, it is assumed that $A_m^{n+1} \approx A_m^n$. In the situation of deposition, usually $\Delta A_{b,j+1} + A_{m,j+1}^n \geq A_{m,j+1}^{n+1}$, then $p_{bk,j+1}^{*n+1} = p_{bk,j+1}^n$, and the error equation for bed-material gradation is

$$\delta^{n+1} = \delta^n \frac{A_{m,j+1}^{n+1} - \Delta A_{b,j+1} - (f_2 - f_1 e_k)(1 - \theta_p) Q_{tk,j+1}^{*n+1}}{A_{m,j+1}^{n+1} + (f_2 - f_1 e_k) \theta_p Q_{tk,j+1}^{*n+1}} \quad (27)$$

where δ = error of bed-material gradation. Numerical stability requires $r = |\delta^{n+1} / \delta^n| \leq 1$, which implies that for the implicit scheme

$$\frac{\theta(1 - e_k) Q_{tk,j+1}^{*n+1} \Delta t}{(1 - p') L_{s,j+1}^{n+1}} \geq \Delta A_{b,j+1} - 2 A_{m,j+1}^{n+1} \quad (28)$$

and for the explicit scheme

$$\frac{\theta(1 - e_k) Q_{tk,j+1}^{*n+1} \Delta t}{(1 - p') L_{s,j+1}^{n+1}} \leq 2 A_{m,j+1}^{n+1} - \Delta A_{b,j+1} \quad (29)$$

In the situation of erosion, usually $\Delta A_{b,j+1} + A_{m,j+1}^n < A_{m,j+1}^{n+1}$, then $p_{bk,j+1}^{*n+1}$ is the bed-material gradation of the sub-surface layer, whose influence on the numerical stability of bed-material gradation of the mixing layer is assumed to be negligible. The error equation for bed-material gradation is

$$\delta^{n+1} = \delta^n \frac{A_{m,j+1}^n - (f_2 - f_1 e_k)(1 - \theta_p) Q_{tk,j+1}^{*n+1}}{A_{m,j+1}^{n+1} + (f_2 - f_1 e_k) \theta_p Q_{tk,j+1}^{*n+1}} \quad (30)$$

from which one can know that the implicit scheme is unconditionally stable, and the numerical stability condition of the explicit scheme is

$$\frac{\theta(1 - e_k) Q_{tk,j+1}^{*n+1} \Delta t}{(1 - p') L_{s,j+1}^{n+1}} \leq A_{m,j+1}^n + A_{m,j+1}^{n+1} \quad (31)$$

In practical calculations, the total bed deformation ΔA_b is usually less than the thickness of the mixing layer, i.e., $|\Delta A_b| \leq A_m^{n+1}$. Considering $e_k < 1$, the condition (28) is automatically satisfied. Conditions (29) and (31) require that the time step Δt has upper bound limits in the explicit scheme. It is obvious that the implicit scheme is much more stable than the explicit scheme.

Requirement of Non-negative Bed-Material Gradation

During the calculation of bed-material gradation, negative values can occur under certain conditions. Of course, this is a nonphysical phenomenon that must be eliminated.

The condition $p_{bk,j+1}^{n+1} \geq 0$ for Eq. (26) implies that

$$f_1 e_{0k} + f_{0k} + [A_{m,j+1}^n - (f_2 - f_1 e_k)(1 - \theta_p) Q_{tk,j+1}^{*n+1}] p_{bk,j+1}^n + (A_{m,j+1}^{n+1} - A_{m,j+1}^n - \Delta A_{b,j+1}) p_{bk,j+1}^{*n} \geq 0 \quad (32)$$

and then

$$\Delta A_{b,j+1} \leq A_{m,j+1}^{n+1} + \frac{f_1 e_{0k} + f_{0k} + A_{m,j+1}^n (p_{bk,j+1}^n - p_{bk,j+1}^{*n})}{p_{bk,j+1}^{*n}} - \frac{\theta(1 - e_k)(1 - \theta_p) Q_{tk,j+1}^{*n+1} \Delta t}{(1 - p') L_{s,j+1}^{n+1}} \frac{p_{bk,j+1}^n}{p_{bk,j+1}^{*n}} \quad (33)$$

Because the last term on the right-hand side of inequality (33) is negative but disappears when $\theta_p = 1$, the implicit scheme can more easily satisfy the requirement of non-negative bed-material gradation than the explicit scheme. Inequality (33) requires that the time step in the explicit scheme be smaller than that in the implicit scheme.

After considering the numerical stability conditions of Preissmann's scheme for the sediment transport equation, constraint (33) can be easily satisfied in the case of the implicit scheme. One of the safest treatments is to impose $\theta = 1$, $|\Delta A_b| \leq A_m^{n+1}$ and $A_m^{n+1} \approx A_m^n$, which is a sufficient but not necessary condition.

Sensitivity of Implicit and Explicit Schemes for Bed-Material Gradation

Assuming $A_{m,j+1}^{n+1} = A_{m,j+1}^n$ in Eq. (26), and differentiating $p_{bk,j+1}^{n+1}$ with respect to $A_{m,j+1}$, one can obtain the following relation:

$$\left(\frac{\partial p_{bk,j+1}^{n+1}}{\partial A_{m,j+1}} \right)_{\theta_p=1} \bigg/ \left(\frac{\partial p_{bk,j+1}^{n+1}}{\partial A_{m,j+1}} \right)_{\theta_p=0} = \left[\frac{A_{m,j+1}}{A_{m,j+1} + f_1(1 - e_k) Q_{tk,j+1}^{*n+1}} \right]^2 \leq 1 \quad (34)$$

The gradient $\partial p_{bk,j+1}^{n+1} / \partial A_{m,j+1}$ represents the change in the calculated bed-material gradation with respect to a variation of the specified mixing layer thickness. Eq. (34) shows that this effect is smaller for the implicit scheme than for the explicit scheme, so that the implicit scheme is less sensitive to $A_{m,j+1}$.

Supplemental Formulas for Sediment Transport

Bank Erosion and Mass Failure

Bed degradation and lateral fluvial erosion of bank toes may cause bank instability, mass failures, and eventual channel widening. The present model simulates erosion of bank toes by using the empirical relationship of Arulanandan et al. (1980). Osman and Thorne's (1988) algorithm is used to analyze the stability of banks, assuming planar failure as the mode of bank failure, with the safety factor being defined as the ratio of the resistance and driving forces for the failure. The eroded bank materials are treated directly as side inflow of sediment in the transport equation (7).

Sediment Transport Capacity

The present model offers four methods for the determination of sediment transport capacity: Wu et al.'s formula (see Wu, Wang and Jia, 2000), the modified Ackers and White's 1973 formula (Proffitt and Sutherland 1983), the modified Engelund and Hansen's 1967 formula (with Wu et al.'s 2000 hiding and exposure correction factor, see Wu and Vieira 2002), and the SEDTRA module (Garbrecht et al. 1995). The SEDTRA module uses three different formulas to calculate sediment transport capacities for different size ranges: Laursen's (1958) formula for size classes from 0.01 to 0.25 mm, Yang's (1973) formula for size classes from 0.25 to 2.0 mm, and Meyer-Peter and Mueller's (1948) formula for size classes from 2.0 to 50.0 mm. Regardless of the formula being used, the hiding and exposure effects of nonuniform sediment are always considered. The availability of multiple formulas in the model enables it to be applied to a wider variety of real-life problems.

Nonequilibrium Adaptation Length L_s

The nonequilibrium adaptation length L_s , which characterizes the distance for sediment to adjust from a nonequilibrium state to an equilibrium state, is a very important parameter in the present model. However, different researchers adopted significantly different values for L_s . Bell and Sutherland (1981) found that L_s relates to time t (in hours) in an experimental case of bed degradation downstream of a dam due to clear water. In numerical modeling, Phillips and Sutherland (1989), Thuc (1991), and Wu et al. (2000) adopted L_s as the average saltation step length of sand on the bed for the laboratory cases, and Rahuel et al. (1989) and Fang (2000) gave L_s much larger values, such as one or twice the numerical grid length, in the case of natural rivers. One reason for the disparity is that L_s is closely related to the dimensions of the studied sediment movements, bed forms, and channel geometry, which are usually markedly different in laboratory and field situations. In laboratory experiments, sediment transport processes are of small scales, such as sand saltation, ripples, and dunes, while in streams, sediment transport processes occur usually at larger scales and with longer periods. Another reason for the adoption of different values is that L_s is an important parameter for numerical stability. As shown in Eqs. (24), (29), and (31), small L_s values require small grid sizes and time steps to insure numerical stability. Large mesh sizes and time steps are usually necessary for the calculation in natural situations with limited computer resources, and thus a large L_s is desired. Therefore, it is understandable that different values of L_s have been adopted in the literature. In the present model, L_s is given different values for bed load and suspended load.

As described above, the nonequilibrium adaptation length, especially for bed load, is related to the dimensions of sediment movements, bed forms, and channel geometry. It is desirable that L_s relate to the dominant bed form or channel geometry. For example, in Bell and Sutherland's (1981) experiment of channel degradation due to clear water, the sediment transport was significantly influenced by the scouring hole of the bed that developed with time, advancing downstream from the inlet. Therefore, L_s is related to the magnitude of scouring hole, and in turn is a function of time t . If there are only sand ripples on the bed, which usually occurs in experimental cases, the nonequilibrium adaptation length for bed load may take the average saltation step length of sand or the length of sand ripples, as was adopted by Phillips and Sutherland (1989), Thuc (1991), and Wu et al. (2000). If sand dunes are the dominant bed form, L_s may take the sand dune

length, which is about 7.3 times of the flow depth (van Rijn 1984). If alternate bars are the dominant bed form, L_s may take the length of alternate bars, which is about 6.3 times of channel width (Yalin 1972). Usually, it is suggested to adopt the sand dune length for L_s for flume cases and the alternate bar length for L_s for field cases.

The nonequilibrium adaptation length of suspended load is given with $L_s = Uh/(\alpha\omega_{sk})$. The coefficient α can be calculated with Armanini and di Silvio's (1988) method or other semi-empirical methods. Values of α calculated from these methods are usually larger than 1. However, in practice, α has been given dramatically different values by many researchers, most of them less than 1. Han (1980) and Wu (1991) suggested $\alpha=1$ for the case of strong erosion, $\alpha=0.25$ for strong deposition, and $\alpha=0.5$ for weak erosion and deposition, as a result of validation tests in many reservoirs and rivers. However, α was given very small values, such as 0.001 in the lower Yellow River (Wei 1990). Wu (1991) and Zhou and Lin (1998) theoretically derived that α could be less than 1 as a comprehensive parameter in the model.

In the proposed model, bed load and suspended load are combined together as bed-material load as described in Eq. (7), and the nonequilibrium adaptation length is given as the larger of the lengths computed for bed load and suspended load.

Model Sensitivity to Nonequilibrium Adaptation Length

The sensitivity of the simulated bed changes to the nonequilibrium adaptation length is analyzed in two experimental cases. One is the degradation experiment performed by Ashida and Michiue (1971), and the other is the aggradation experiment conducted by Seal et al. (1995).

Ashida and Michiue's (1971) degradation experiment was performed in a flume 0.8 m wide and 20 m long. The flume bed was filled with nonuniform sediment with a median size of 1.5 mm and standard deviation of 3.47. Clear water was pumped into the flume entrance at a constant discharge. The flow discharge was $0.0314 \text{ m}^3/\text{s}$, and the initial bed slope was 0.01. The computational grid consists of 40 elements with equal length of 0.5 m, and the time step is 10 s. In the experiment, the bed was initially flat, and bed forms developed gradually until a fully developed bed was attained. In order to account for the changes in bed roughness, bed form heights are assumed to vary linearly with time. The time needed to complete the bed form development process is assumed as about 60 min. The Manning's n for the flume bed in the final stage is about 0.023. Wu et al.'s (2000) formula is used to determine the sediment transport capacity, while the mixing layer thickness is set as the median size of original sediment mixture.

To show the influence of L_s on the simulated results, several functions ($L_s = 7.3h$, $L_s = t$, and $L_s = 1 + 0.5t$) are tested. Here, t is time in hours. Fig. 2 shows the comparison of the measured and calculated bed scour depths at 7, 10, and 13 m upstream from the weir. The calculated scour depths agree well with the experimental data. The trends of intensive scour in the initial period and weak scour in the final equilibrium stage are very well reproduced. The function $L_s = 7.3h$ provides the best result for the bed scouring process, especially in regard to the time to achieve equilibrium scour. The results for $L_s = t$ and $L_s = 1 + 0.5t$ are also very close to the measured data, showing that the calculated scour depth is not very sensitive to L_s .

Seal et al.'s (1995) aggradation experiment was conducted in a flume 45 m long and 0.305 m wide, with an initial bed slope of

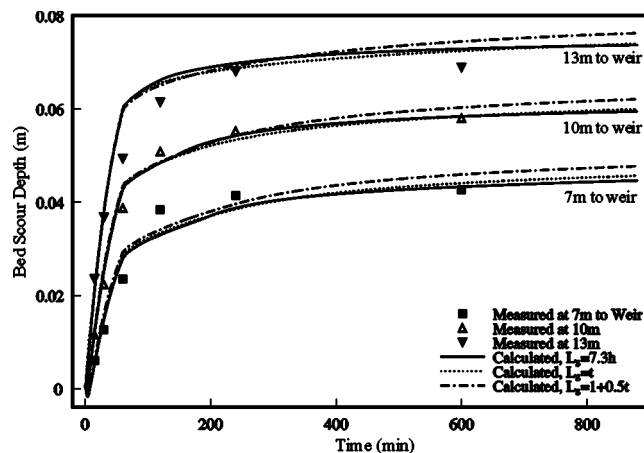


Fig. 2. Measured and calculated bed scour depths in Ashida and Michiue's experiment

0.002. The tailgate was kept at a constant height so that an undular hydraulic jump was produced at the downstream end of the main gravel deposit. The sediment fed at the flume entrance was a weakly bimodal mixture comprising a wide range of sizes from 0.125 to 64 mm. Due to sediment overloading, an aggradational wedge developed, its front gradually moving downstream while the upstream bed elevation continued to rise. The model is used to simulate experimental run 2. The water discharge is $0.049 \text{ m}^3/\text{s}$, the sediment feed rate is $5.65 \text{ kg}/\text{min}$, and the tailgate water elevation is 0.45 m. The computational domain consists of 90 intervals with uniform spacing of 0.5 m. The time step is 30 s. The mixing layer thickness is half the sand dune height. The adaptation length L_s is set as 0.5 m, 2 m, and $7.3h$. Here, h is the average flow depth over the wedge, and $7.3h$ is approximately 1 m. Fig. 3 provides a comparison of the measured and predicted bed profiles at various times. The results show that L_s has obvious impact on the slope of the deposit front. The longer the adaptation length, the smaller the front slope. However, L_s has only a limited influence on the top slope of the wedge as well as on the location and height of the wedge front.

The above analyses show that $L_s = 7.3h$ gives very promising predictions in both degradation and aggradation cases. However,

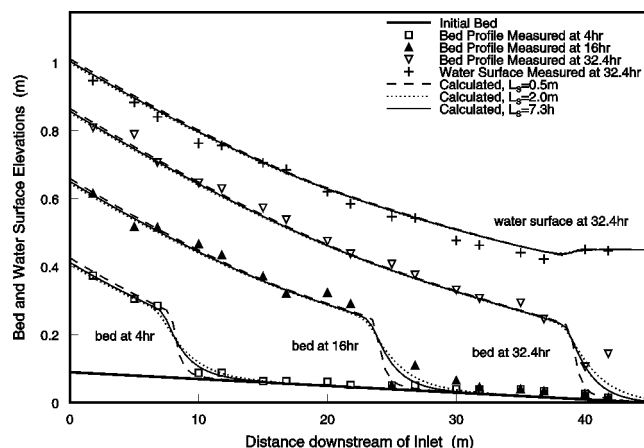


Fig. 3. Measured and calculated bed profiles in the experiment by (Seal et al.'s 1995).

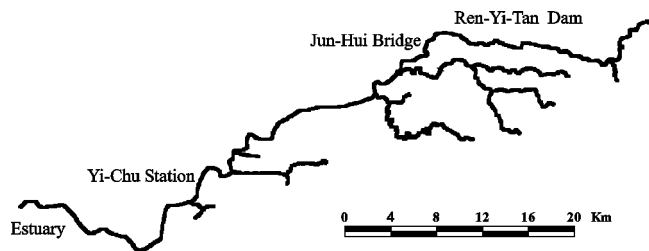


Fig. 4. Sketch of the Pa-Chang River

this is only for bed load in flume cases. For other cases L_s may take different values as described in the previous section.

In addition, it has been also found that the proposed model is insensitive to time step and grid spacing. However, the evaluation of the mixing layer thickness is very important for the simulation of channel armoring process. For details, refer to Wu and Vieira (2002).

Model Applications

Bed Morphological Changes in the Pa-Chang River

The Pa-Chang River is an important river in south Taiwan. It is 80 km long, with a drainage basin of 475 km². The 36.1-km-long study reach terminates at the Yi-Chu Station, 15.9 km upstream of the river estuary, as shown in Fig. 4. The channel slope is gentle in the lower part of the study reach but steep in the upper part. Seventy-seven cross sections are used to represent the study reach. An open boundary condition is specified at the outlet. The study reach receives eight tributaries that are not part of the simulation, but their water and sediment discharges are considered as side inflows into the main channel. The bed load L_s is set as the alternate bar length. The computation time step is 2.5 min.

Fig. 5 shows the comparison of the measured and simulated flow discharges at the Jun-Hui Bridge Station for selected storms between 1995 and 1998. The model predicts the flow discharges very well. Fig. 6 shows the comparison between the calculated and measured thalweg changes in the upper part of the study reach for the same period. Three sediment transport capacity formulas are used: the SEDTRA module, Wu et al.'s formula, and the modified Engelund and Hansen's formula. The large erosion is well reproduced.

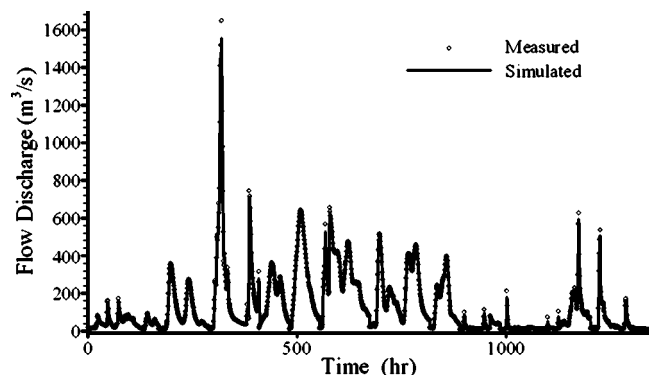


Fig. 5. Flow discharges in Jun-Hui bridge of the Pa-Chang River

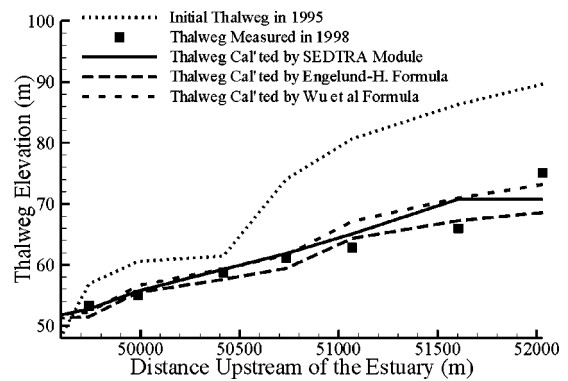


Fig. 6. Thalweg changes in the study reach of the Pa-Chang River

Sediment Transport in the Goodwin Creek Watershed

The drainage area of Goodwin Creek watershed in Mississippi is 21.3 km². Most channels are ephemeral, with perennial flows occurring only in the lower reaches of the watershed. The average channel slope is 0.004. The runoff produced by storm events swiftly exits the watershed, and the discharge returns to baseflow levels within one to three days. The sediments being transported in the channels range from silt (<0.062 mm) to sand to gravel (<65 mm). Fourteen fully instrumented flumes were constructed in the channels to control degradation of the channel bed and to monitor runoff and sediment yield.

The present model is used to simulate the channel changes from 1978 to 1995. The channel network of Goodwin Creek, shown in Fig. 7, is extracted from the elevation data of a Digital Elevation Model. A computational mesh consisting of 253 cross sections is obtained by refining this extracted channel network and including ten in-stream measuring flumes and four culverts located in channels of second Strahler order or above. The daily runoff and sediment yield from the upland fields of the 138 sub-basins due to a total of 1192 storm events, which were simulated by Bingner et al. (1997) with the watershed model SWAT, are converted into triangular hydrographs and sedigraphs that describe inflows to the nodes of the channel network. Nine size classes are used to represent the nonuniform sediment mixture. The simulation considers toe erosion and mass failure of the banks. The bed load L_s is defined as 6.3 times the average channel width for each channel. The time step in the channel simulation is 15 min. The execution time is about 1 h on a 2 GHz PC.

Fig. 8 shows the comparison of the calculated and measured thalweg changes between flumes No. 1 and No. 2, from 1978 to

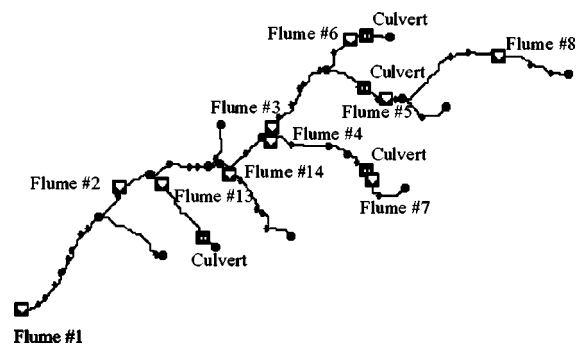


Fig. 7. Sketch of the channel network of the Goodwin Creek watershed

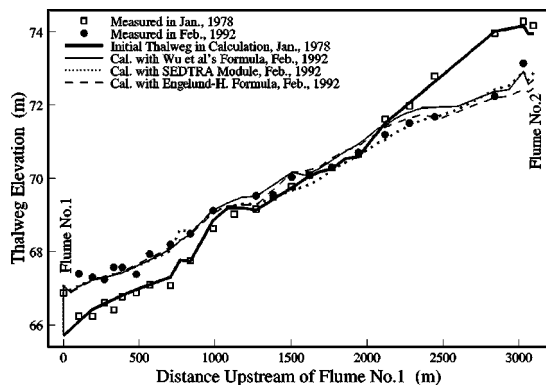


Fig. 8. Thalweg changes between flumes No. 1 and No. 2 in the Goodwin Creek

1992. The calculated results are obtained by using three sediment transport capacity formulas: Wu et al.'s formula, the SEDTRA module, and the modified Engelund and Hansen's formula. The model predicts well the scour and deposition pattern that takes place between flumes No. 1 and 2. Fig. 9 shows the comparison of the calculated and measured annual sediment yields at the watershed outlet (measuring flume No. 1). The present model provides calculated results that are close to the field measurements.

Conclusions

This paper presents a one-dimensional model for the simulation of flow and sediment transport in dendritic channel networks. The flow model calculates unsteady flows in open channels with compound cross sections using the well-proven Preissmann method and Thomas algorithm. The inclusion of methods for the solution of unsteady flows through a variety of structures allows the model to account for their effects on flow, sediment transport, and channel morphological changes.

The proposed model adopts a nonequilibrium transport model for nonuniform sediment. The sediment transport capacity is determined by four formulas, which have considered the hiding and exposure effect among different size classes. Although the sediment calculation is decoupled with the flow simulation, the sediment module solves the discretized equations of sediment transport, bed changes, and bed-material sorting in a coupled fashion through a direct method, which ensures that the computation cost of the coupled model remains at the same level as that of the fully

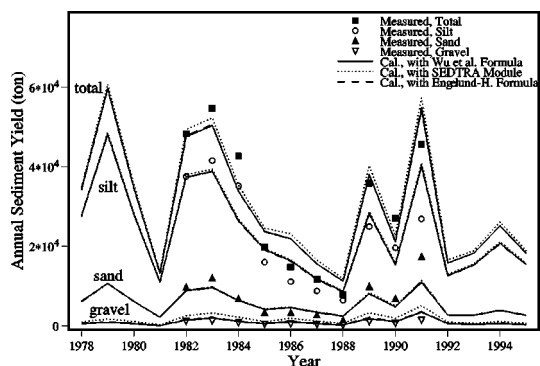


Fig. 9. Sediment yields at flume No. 1 in the Goodwin Creek

decoupled model at each time step, and the overall computation efficiency increases significantly. The analysis of the method reveals that its solution is more stable and less sensitive to the choice of model parameters when compared to the traditional fully decoupled model.

The model is tested in several real-life cases. The model is able to determine sediment transport and morphological changes in channel networks, and to evaluate the effect of in-stream hydraulic structures in a long time period.

Acknowledgments

The present model is part of the research project sponsored by the USDA Agricultural Research Service Specific Research Agreement No. 58-6408-2-0062. The watershed simulation results for the Goodwin Creek watershed were provided by Dr. R. Bingner, USDA-ARS National Sedimentation Laboratory. The data for the Pa-Chang River were provided by Professors H.-M. Hsia and C.-C. Cheng, Taiwan.

References

- Ackers, P., and White, W. R. (1973). "Sediment transport: A new approach and analysis." *J. Hydraul. Div., Am. Soc. Civ. Eng.*, 99(11), 2041–2060.
- Armanini, A., and Di Silvio, G. (1988). "A one-dimensional model for the transport of a sediment mixture in non-equilibrium conditions." *J. Hydraul. Res.*, 26(3), 275–292.
- Arulanandan, K., Gilligley, E., and Tully, R. (1980). "Development of a quantitative method to predict critical shear stress and rate of erosion of naturally undisturbed cohesive soils." *Rep. GL-80-5*, U.S. Army Engineers Waterway Experiment Station, Vicksburg, Miss.
- Ashida, K., and Michiue, M. (1971). "An investigation of river bed degradation downstream of a dam." *Proc., 14th Congress of the IAHR*, Paris, 3, 247–256.
- Bell, R. G., and Sutherland, A. J. (1983). "Nonequilibrium bed load transport by steady flows." *J. Hydraul. Eng.*, 109(3), 351–367.
- Bingner, R. L., Alonso, C. V., Arnold, J. G., and Garbrecht, J. (1997). "Simulation of fine sediment yield within a DEC watershed." *Proc., Conf. on Management of Landscapes Disturbed by Channel Incision*, The University of Mississippi, University, Miss., 1106–1110.
- Cao, Z., Day, R., and Egashira, S. (2002). "Coupled and decoupled numerical modeling of flow and morphological evolution in alluvial rivers." *J. Hydraul. Eng.*, 128(3), 306–321.
- Chang, H. H. (1982). "Mathematical model for erodible channels." *J. Hydraul. Div., Am. Soc. Civ. Eng.*, 108(5), 678–689.
- Correia, L., Krishnappan, B. G., and Graf, W. H. (1992). "Fully coupled unsteady mobile boundary flow model (FCM)." *J. Hydraul. Eng.*, 118(3), 476–494.
- Cui, Y., Parker, G., and Paola, C. (1996). "Numerical simulation of aggradation and downstream fining." *J. Hydraul. Res.*, 34(2), 185–204.
- Cunge, J. A., Holly, F. M., Jr., and Verwey, A. (1980). *Practical aspects of computational river hydraulics*, Pitman Publishing Inc., Boston.
- Engelund, F., and Hansen, E. (1967). *A monograph on sediment transport in alluvial streams*, Teknisk, Copenhagen, Denmark.
- Fang, H. W. (2000). "Three-dimensional calculations of flow and bed-load transport in the Elbe river." *Report No. 763*, Institute for Hydro-mechanics, University of Karlsruhe, Germany.
- Garbrecht, J., Kuhnle, R., and Alonso, C. (1995). "A sediment transport capacity formulation for application to large channel networks." *J. Soil Water Conservat.*, 50(5), 527–529.
- Han, Q. W. (1980). "A study on the nonequilibrium transportation of suspended load." *Proc., 1st Int. Symp. on River Sedimentation*, Beijing.

- Holly, Jr., F. M., and Rahuel, J. L. (1990). "New numerical/physical framework for mobile-bed modeling, Part I: Numerical and physical principles." *J. Hydraul. Res.*, 28(4), 401–416.
- Kassem, A., and Chaudhry, M. H. (1998). "Comparison of coupled and semicoupled numerical models for alluvial channels." *J. Hydraul. Eng.*, 124(8), 794–802.
- Langendoen, E. J. (1996). Discretization diffusive wave model. *Technical Report No. CCHE-TR-96-1*, Center for Computational Hydroscience and Engineering, The University of Mississippi, University, Miss.
- Laursen, E. (1958). "The total sediment load of streams." *J. Hydraul. Div., Am. Soc. Civ. Eng.*, 54(1), 1–36.
- Lai, C. (1991). "Modeling alluvial channel flow by multimode characteristics method." *J. Hydraul. Eng.*, 117(1), 32–53.
- Lyn, D. A., and Goodwin, P. (1987). "Stability of a general Preissmann scheme." *J. Hydraul. Eng.*, 113(1), 16–28.
- Meselhe, E. A., and Holly, F. M., Jr. (1993). "Simulation of unsteady flow in irrigation canals with dry bed." *J. Hydraul. Eng.*, 119(9), 1021–1039.
- Meyer-Peter, E., and Mueller, R. (1948). "Formulas for bed-load transport." *Rep. on 2nd Meeting of IAHR*, Stockholm, Sweden, 39–64.
- Osman, A. M., and Thorne, C. R. (1988). "Riverbank stability analysis, I: Theory." *J. Hydraul. Eng.*, 114(2), 134–150.
- Phillips, B. C., and Sutherland, A. J. (1989). "Spatial lag effects in bed load sediment transport." *J. Hydraul. Res.*, 27(1), 115–133.
- Preissmann, A. (1961). "Propagation des intumescences dans les canaux et Les Rivières." *1 Congres de l'Association Francaise de Calcul*, Grenoble, France.
- Proffit, G. T., and Sutherland, A. J. (1983). "Transport of nonuniform sediment." *J. Hydraul. Res.*, 21(1), 33–43.
- Rahuel, J. L., Holly, F. M., Chollet, J. P., Belleudy, P. J., and Yang, G. (1989). "Modeling of riverbed evolution for bedload sediment mixtures." *J. Hydraul. Eng.*, 115(11), 1521–1542.
- Saiedi, S. (1997). "Coupled modeling of alluvial flows." *J. Hydraul. Eng.*, 123(5), 440–446.
- Seal, R., Parker, G., Paola, C., and Mullenbach, B. (1995). "Laboratory experiments on downstream fining of gravel, narrow channel runs 1 through 3: supplemental methods and data." *External Memorandum M-239*, St. Anthony Falls Hydraulic Lab., University of Minnesota, Minneapolis.
- Thomas, W. A. (1982). "Chapter 18: Mathematical modeling of sediment movement." *Gravel-bed rivers*, R. D. Hey et al., eds., Wiley, New York.
- Thuc, T. (1991). "Two-dimensional morphological computations near hydraulic structures." doctoral dissertation, Asian Institute of Technology, Bangkok, Thailand.
- Tsai, C. T., and Yen, C. L. (1982). "Simulation of unsteady flow in movable bed channel." *Proc., 3rd Congress of Asian and Pacific Regional Division, IAHR*, Bandung, Indonesia.
- van Rijn, L. C. (1984). "Sediment transport, part III: Bed forms and alluvial roughness." *J. Hydraul. Eng.*, 110(12), 1733–1754.
- van Niekerk, A., Vogel, K. R., Slingerland, R. L., and Bridge, J. S. (1992). "Routing of heterogeneous sediments over movable bed: Model development." *J. Hydraul. Eng.*, 118(2), 246–262.
- Venutelli, M. (2002). "Stability and accuracy of weighted four-point implicit finite difference schemes for open channel flow." *J. Hydraul. Eng.*, 128(3), 281–288.
- Wei, Z. L. (1990). "Horizontal 2-D numerical model of flow and sediment transport in the lower Yellow River." Wuhan Univ. of Hydraulic and Electric Engineering, Wuhan, China.
- Wu, W. (1991). "The study and application of 1-D, horizontal 2-D and their nesting mathematical models for sediment transport." PhD Dissertation, Wuhan Univ. of Hydraulic and Electric Engineering, Wuhan, China.
- Wu, W., Rodi, W., and Wenka, T. (2000). "3-D numerical modeling of water flow and sediment transport in open channels." *J. Hydraul. Eng.*, 126(1), 4–15.
- Wu, W., and Vieira, D. A. (2002). "One-dimensional channel network model CCHE1D 3.0-Technical manual." *Technical Rep. No. NCCHE-TR-2002-1*, National Center for Computational Hydroscience and Engineering, The University of Mississippi, University, Miss.
- Wu, W., Wang, S. S.-Y., and Jia, Y. (2000). "Nonuniform Sediment Transport in Alluvial Rivers." *J. Hydraul. Res.*, 38(6), 427–434.
- Yalin, M. S. (1972). *Mechanics of sediment transport*, Pergamon, New York.
- Yang, C. T. (1973). "Incipient motion and sediment transport." *J. Hydraul. Div., Am. Soc. Civ. Eng.*, 99(10), 1679–1704.
- Zhou, J., and Lin, B. (1998). "One-dimensional mathematical model for suspended sediment by lateral integration." *J. Hydraul. Eng.*, 124(7), 712–717.